Eur. Phys. J. E (2012) **35**: 132
DOI 10.1140/epje/i2012-12132-8

THE EUROPEAN PHYSICAL JOURNAL E

Regular Article

Film thickness dependent ordering dynamics of lamellar forming diblock copolymer thin films

Robert D. Peters and Kari Dalnoki-Veress[a]

Department of Physics & Astronomy and the Brockhouse Institute for Materials Research, McMaster University, Hamilton, Canada

Received 2 August 2012 and Received in final form 19 October 2012
Published online: 19 December 2012 –

Abstract. Ellipsometry is used in a novel way to study the ordering dynamics of symmetric poly(styrene-methyl methacrylate) diblock copolymer thin films. Ordered thin films form lamellae parallel to the substrate which can form islands or holes at the free surface to ensure commensurability of the layers. The sensitivity of ellipsometry provides the unique ability to probe morphological changes during the ordering process *before* the ultimate formation of islands or holes at the free surface. We observe three distinct stages in the ordering process: i) an ordering into an intermediate state, ii) an incubation time where the film structure remains constant and iii) the nucleation of islands or holes to achieve equilibrium lamellar morphology. The time-resolved measurement of an incubation period and initial ordering stage provides a means for studying the effect of thickness on the ordering kinetics. The dependence of incubation time on the commensurability of the initial film height is explained using strong segregation theory.

1 Introduction

Diblock copolymers consist of two chemically distinct polymer chains that are covalently bonded together. These molecules are known for their remarkable ability to self-assemble into complex structures when annealed below the order disorder transition (ODT) [1]. Thin films of diblock copolymers are of particular interest due to their promise of technological advancement in photonics [2], data storage [3,4], adhesion [5], and surface property modification [6] among other applications [2].

It has been well established that symmetric diblocks, one of the simplest copolymers consisting of equal parts of both polymer blocks, will microphase separate into a lamellar morphology [1]. In equilibrium, each copolymer bilayer will have a characteristic thickness L_0, determined by the balance between the enthalpic cost of creating the lamellar interfaces and the entropic cost of chain stretching [1]. In uncapped, supported thin films, we must take into account the effect of additional interfaces resulting from the substrate and free surface. A difference in the interfacial energies of the two polymer blocks with the substrate and the air causes the orientation of lamellae parallel to these interfaces [7]. In asymmetric wetting conditions, interfacial energies are such that one block preferentially orders at the air interface and the other block at the substrate, as is the case for poly(styrene-methyl methacrylate) (PS-PMMA). This results in a total film thickness at equilibrium that is $(N + 1/2)L_0$, with N an integer. This film height preserves the bilayer thickness L_0 while satisfying the surface preferences for both interfaces [8].

When the initial film height, h_0, is incommensurate (*i.e.* $h_0 \neq (N + 1/2)L_0$), the free surface will form relief structures of islands or holes upon annealing. These relief structures will grow, conserving volume, until the entire film is composed of two distinct heights, both satisfying the equilibrium condition of $h = (N + 1/2)L_0$ [8]. Though the equilibrium structure of symmetric diblock films is well understood [7,8], how the films order remains an elusive question. A number of studies have examined the growth of islands or holes both experimentally [9–12] and theoretically [9,13] to discern how a symmetric diblock film evolves when annealed below the ODT. Though these studies provide a good picture of how islands and holes form and grow, to the best of our knowledge, time-resolved *in situ* measurements of film ordering *before* the free surface forms relief structures are yet to be presented. Using ellipsometry, a tool that is sensitive to the small changes in structure within the film, we investigate the timescales of evolution from amorphous to lamellar morphologies of symmetric PS-PMMA thin films.

2 Experiment

2.1 Ellipsometry

In previous work, nulling ellipsometry has proven effective for measuring diblock morphological changes [14]. In the form of nulling ellipsometry employed here, circularly polarised monochromatic light is passed through a polarizer

[a] e-mail: dalnoki@mcmaster.ca

and quarter wave plate such that when the polarizer is set at angle P, the elliptically polarized light produced after reflection from the film will be linearly polarized. A second polarizer called the analyzer is then rotated to an angle A such that it is cross polarized with the resultant light, yielding a minimum or "null" intensity. In traditional ellipsometry, these polarizer angles P and A are used to calculate film properties such as thickness and index of refraction of a thin film through the standard equations of ellipsometry [15]. Unfortunately, this analysis is model dependent, thus requiring a knowledge of the film structure. Since the evolution of symmetric diblock films from amorphous to lamellar structure is complex and annealing time dependent [16–18], such a direct analysis would be speculative.

To utilize the sensitivity of ellipsometry while simplifying our analysis, we use a modified ellipsometry technique for the bulk of our measurements. The approach we take may not be easily invertible to direct structural information, but as we will see, can be used to obtain the kinetics of changes in the properties of the sample. When the diblock films are annealed, the polarizer angles P and A are fixed to the settings that create a null intensity at the very beginning of the annealing process. Upon annealing, the diblock film will order from the amorphous structure obtained after sample preparation with an average index of refraction and no internal interfaces, to a lamellar morphology with interfaces between layers of PS and PMMA. Since our polarizer angles remain fixed throughout the annealing process, even a small change in the index of refraction profile within the film will alter the reflected polarization of light, causing a change in the measured intensity [14]. Studying the change in the intensity during film evolution, we can measure the timescales associated with the ordering of lamellar forming thin films before the formation of islands or holes occurs at the free surface. The high sensitivity of ellipsometry to changes in the index of refraction profile makes this experimental tool ideal for studying the ordering of the symmetric diblock.

2.2 Sample preparation

PS-PMMA of molecular weight $M_w = 25000$–$26000\,\mathrm{g/mol}$ and a polydispersity of 1.06 was used in this study (Polymer Source, Canada). Thin films with thicknesses varying from $h_0 = 105$ to 195 nm were spincoated from dilute toluene solutions (2.5–4.5% by mass) onto silicon with a 1.7 nm native oxide layer. The initial as-cast thicknesses ranged from $h_0 \sim 4.0L_0$ to $7.3L_0$, with $L_0 = 26.5\,\mathrm{nm}$ as measured by AFM for the PS-PMMA molecules used in this study. Samples were then heated in vacuum at 80 °C for 2 hours to remove residual solvent and initial film heights were measured using ellipsometry (Accurion Nanofilm EP3, Germany). Samples were annealed during the ellipsometry experiment on a modified microscope heating stage (Linkam THMS 600, United Kingdom). A rapid heating rate of 90 °C/min was used for all measurements.

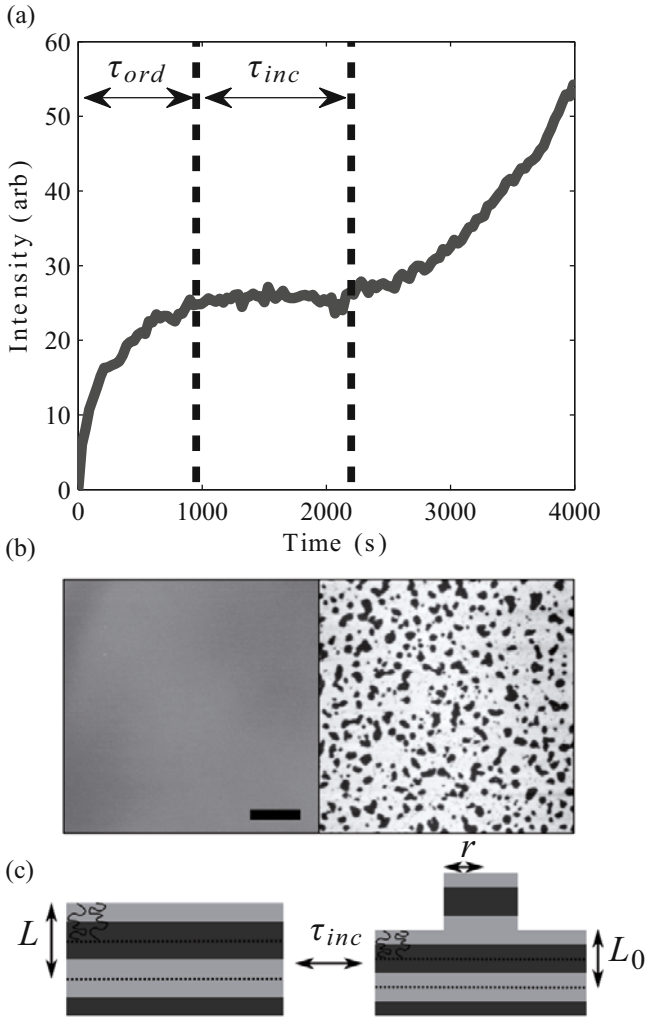

Fig. 1. a) The result of a typical intensity measurement taken for a 137 nm ($5.17L_0$) film with annealing temperature of 160 °C. b) AFM topography images of 141 nm ($5.32L_0$) sample taken in the plateau region (left) and after the second intensity increase (right). Scale bar is 10 μm. Both images have the same height scale of 28 nm. c) Schematic of transition from metastable lamellar morphology in plateau region to final equilibrium state.

3 Results and discussions

In our experiments, the thin films were rapidly heated above the glass transition and below the ODT. The ellipsometric angles were immediately rotated to achieve a null intensity after the analyzer, and the intensity was monitored using the fixed-angle ellipsometry technique described above. A typical intensity profile, shown in fig. 1a, can be separated into three stages: i) an initial intensity increase, ii) a plateau region, followed by iii) another intensity increase. Using atomic force microscopy (AFM), we have observed that the surface remains flat with peak-to-peak roughness less than 1 nm until the second intensity increase, stage iii). Thus, the second intensity increase is caused by the onset of island or hole formation at the free surface. An example of typical AFM measurements of a

film in the plateau region and after the second intensity increase is provided in fig. 1b. The combination of AFM and the ellipsometry measurements indicate that two distinct processes occur before any changes to the surface topography caused by the final formation of islands or holes. First, an initial ordering of the film, signified by the first intensity increase and the time $\tau_{\rm ord}$. Second, a plateau region indicating that the optical properties within the film remain unchanged (within the resolution of the experiment), represented by the time $\tau_{\rm inc}$. The plateau region is a direct measurement of the incubation period in a metastable state prior to the nucleation event associated with the formation of islands or holes.

The incubation time is not a new concept in the organization of symmetric diblock films [9,10,12] and is to be expected if there is a metastable intermediate morphology. The system can be metastable because of an activation barrier associated with the cost of creating excess surface at the edge of islands or holes —directly analogous to the nucleation and growth regime in phase separation. The fixed-angle ellipsometry technique provides the ability to distinguish between the initial ordering stage and the incubation period during film organization with excellent time resolution. This ability to measure the two timescales separately provides the unique opportunity to study the effect of thickness and commensurability on both $\tau_{\rm ord}$ and $\tau_{\rm inc}$ over a wide range of thicknesses. These timescales and their dependence on initial thickness also provide insight into the intermediate metastable morphology and ordering pathway for symmetric diblock thin films.

In the initial ordering of symmetric diblock thin films, it has been well established that bilayer formation will begin at the interfaces due to strong surface energy differences between the two polymer blocks [16–18]. In the case of PS-PMMA, the surface energy of PMMA at the substrate interface is much lower than that of PS due to hydrogen bonding at the native oxide layer [18,19]. Conversely, PS has only a slightly lower surface energy than PMMA at the air interface, only differing by $\sim 1\%$ [20]. Thus, as the film begins to order, the difference in surface energy at the substrate will initiate ordering from that interface propagating toward the free surface, forming bilayers of thickness $\sim L_0$ [16,18]. For incommensurate films, as ordering nears completion there will be either an excess or deficiency of material which prevents lamellae from achieving equilibrium bilayer thicknesses throughout the film. This incommensurability is what will eventually drive nucleation of islands or holes. Using the measurement of the temperature dependence of the PS-PMMA ODT from [21], we calculate the interaction parameter to be $\chi N \sim 27$ for the PS-PMMA in this study when accounting for compositional fluctuations [22]. Thus, the remaining amorphous polymer at the free interface is unstable [23], requiring ordering into an intermediate state. Metastable intermediate states with parallel lamellae of non-equilibrium width have been shown to exist before island or hole nucleation in lamellar-forming diblock films through the use of neutron reflectivity [9]. For a film that is slightly thicker than commensurate, this means that the already formed lamellae must incorporate the excess amorphous material, deforming into bilayers of thickness $L \geq L_0$. This process will conserve material and lamellar order while forming an intermediate state with a flat film surface. Conversely, if the initial film height is slightly thinner than commensurate, the intermediate state will consist of bilayers of $L \leq L_0$.

While it is not clear how the system adjusts to incorporate amorphous material with non-ideal thickness, we can turn to a simple free-energy calculation to understand the lamellar organization. We calculate the free energy of the film morphology in the strong segregation limit (SSL) [24] for a general film thickness without requiring commensurability (note that the model presented below should be interpreted as a first-order approximation). In the SSL, the lowest free-energy morphology in the intermediate state is that of lamellae with equal bilayer thickness. In this morphology, the excess or deficit of polymer in an incommensurate film is shared between all lamellae, decreasing the total free energy of the film. This morphology of equally deformed lamellae is metastable and consistent with previous measurements of film structure in the intermediate ordered state [9]. In this metastable state, each bilayer will have a thickness of

$$L = \frac{h_0}{\left(N + \frac{1}{2}\right)}, \tag{1}$$

schematically shown in fig. 1c. Then, for films with $h_0 < (N + 1/2)\, L_0$, the metastable state would exhibit bilayers that are equally compressed, at a cost of increasing the interaction between the two blocks. In contrast, for films with $h_0 > (N + 1/2)\, L_0$, the metastable state consists of equally swollen bilayers, with an associated cost of stretching the polymers further than in the equilibrium state. Such swollen or compressed bilayers are equivalent to the equilibrium conformation of films confined between two hard walls which has been studied before [25].

The ordering time $\tau_{\rm ord}$ (see fig. 1) represents the time required to form the intermediate state. To study the effect of thickness on $\tau_{\rm ord}$, we measured the initial ordering process at 155 °C, where $\tau_{\rm ord} > 5$ hours for the film heights used in our study. We performed a conventional nulling ellipsometry measurement where we measure the P and A necessary to create a null intensity as two nearly commensurate films of 146 nm ($\sim 5.55 L_0$) and 174 nm ($\sim 6.56 L_0$) order into the metastable state. Just as in the case of the intensity profile in fixed angle ellipsometry experiments, we do not attempt to model the ellipsometry data. Rather, for determination of the kinetics of ordering it suffices to recognise that if the ellipsometric angles are changing with time, so must the internal structure. $P(t)$ and $A(t)$ change for a time $\tau_{\rm ord}$, and then plateau as the film reaches the metastable state. In fig. 2, we see that the $6.56 L_0$ film takes ~ 7 hours to reach the plateau region, whereas the $5.55 L_0$ film takes ~ 5 hours. As both films exhibit similar incommensurabilities ($\sim 0.05 L_0$ larger than commensurate height), this increase in ordering time for the thicker film can be attributed to the time needed to order an additional bilayer. The fractional change in $A(t)$ for the 174 nm film is a demonstration of the complex ellipsometric response with changing film structure that occurs

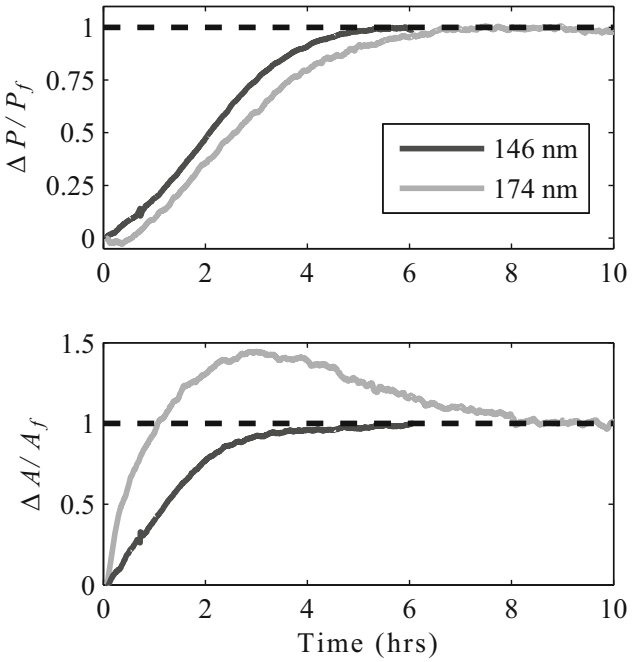

Fig. 2. Nulling ellipsometry measurement of the fractional change in nulling polarizer ($\Delta P/P_f$) and analyzer ($\Delta A/A_f$) angles during the initial ordering stage of 146 nm ($\sim 5.5L_0$) and 174 nm ($\sim 6.5L_0$) films. P_f and A_f represent the nulling polarizer and analyzer angles in the intermediate state.

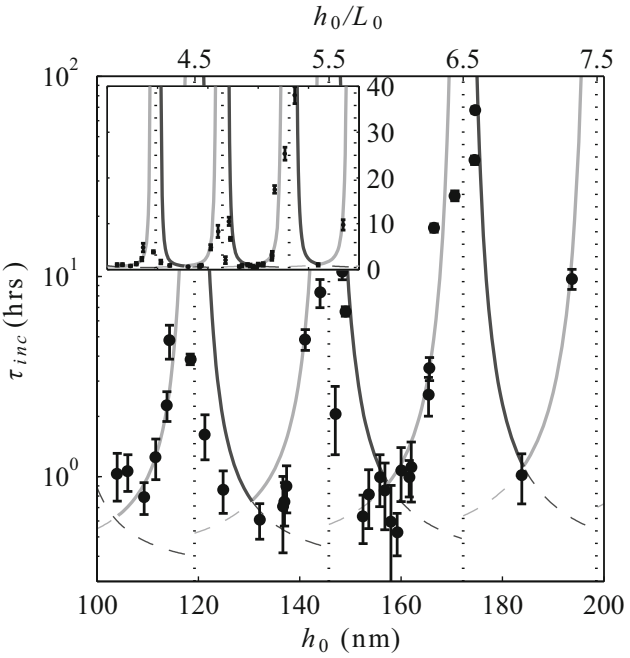

Fig. 3. Incubation time as a function of initial film height on a log-linear scale. The model incubation times for the growth of islands (dark grey) or holes (light grey) are given for each lamellar region. The inset displays the same results on a linear-linear scale. The dotted lines represent commensurate thicknesses of $(N + 1/2)L_0$.

upon initial ordering. As the formation of bilayers propagates toward the free surface, the response of P and A is not necessarily a monotonic function for all films, however as we are simply identifying the timescale associated with approaching a region of no change, this does not affect our evaluation of the ordering time, $\tau_{\rm ord}$.

For the remaining measurements, samples were annealed at 160 °C and characterized with fixed-angle ellipsometry measurements. At this higher temperature the samples order into the metastable state much faster, with $\tau_{\rm ord} \sim 20$ minutes. The incubation time $\tau_{\rm inc}$, corresponding to the time the samples remain in the metastable state, was analyzed and defined as the time for which the intensity profile varied by $< 10\%$ from the plateau intensity of the metastable state (See fig. 1a). As an added precaution, during the experiment the samples were also imaged using optical microscopy, ensuring that the end of the incubation of the metastable state coincides with the optically observable nucleation of islands or holes at the film surface.

While the changes in $\tau_{\rm ord}$ with h_0 at 160 °C are too small to measure, the measured incubation times, $\tau_{\rm inc}$, of nearly commensurate films increase by over 2 orders of magnitude (see fig. 3). This significant dependence of $\tau_{\rm inc}$ on h_0 is to be expected. Consider the case of a commensurate film which can order into lamellae with bilayer thickness L_0, with no need to swell or compress lamellae. This results in no driving force for nucleation of islands or holes, thus the incubation time diverges. In contrast, for incommensurate films the further the film is from commensurability, the further the bilayers are from equilibrium in the metastable state. Thus, the driving force to nucleate islands or holes increases and $\tau_{\rm inc}$ decreases.

4 Model

A simple model calculated in the SSL can elucidate the dependence of incubation time on h_0. Let us first consider the case where the film is initially slightly thicker than commensurate. For this case, $L > L_0$ in the metastable state and islands must form to reduce the lamellae to their equilibrium spacing while conserving volume. If we assume a local model, where the formation of an island initially only affects the top bilayer of the metastable film morphology as shown in fig. 1c, then the free-energy change will be a combination of surface energy cost due to the formation of an island edge and a free-energy decrease due to the formation of lamellae with the equilibrium thickness L_0. The change in free energy may be written as

$$\Delta F = 2\pi r\sigma + V \cdot \Delta G_V(L), \qquad (2)$$

where r is the radius of the island grown at the free surface, σ is the line tension of the island edge, V is the local volume of the film participating in the formation of the island, and $\Delta G_V(L)$ is the free-energy change per unit volume for lamellae to go from a lamellar spacing of L to L_0.

Using conservation of volume between initial and final states, we can define the local volume as $V = \pi r^2 L_0 L/\delta L$,

where $\delta L = L - L_0$. Differentiating the free energy with respect to island radius, finding a critical radius for island formation, and substituting the critical radius back into eq. (2), we obtain an energy barrier for nucleation of

$$\Delta F^* = \frac{-\pi\sigma^2}{\Delta G_V} \cdot \frac{\delta L}{L_0 L}. \tag{3}$$

In the SSL, the difference between the initial and final state entropic and enthalpic contributions is given by [24]

$$\Delta G_V = \left(\frac{\gamma}{L_0} + \alpha L_0^2\right) - \left(\frac{\gamma}{L} + \alpha L^2\right), \tag{4}$$

where γ is the interfacial tension at the PS-PMMA interfaces and the constant $\alpha = kT/(N^2a^5)$, with polymerization index N and monomeric lengthscale a.

At the equilibrium condition $(\mathrm{d}G_V/\mathrm{d}L)|_{L_0} = 0$, and thus $\gamma = 2\alpha L_0^3$. In combination with eq. (3), this equation yields a free-energy barrier to nucleation of

$$\Delta F^* = \frac{\pi\sigma^2}{3\alpha L_0^2 \delta L + \alpha L_0 (\delta L)^2}. \tag{5}$$

Therefore, the incubation time may be calculated as

$$\tau_{\mathrm{inc}} = \tau_0 \exp\left(\frac{\Delta F^*}{kT}\right) = \tau_0 \exp\left(\frac{\beta}{\delta L + \frac{\delta L^2}{3L_0}}\right), \tag{6}$$

where τ_0 and β are fitting constants with $\beta \equiv \pi\sigma^2/(3kT\alpha L_0^2)$. The constant τ_0 governs the dynamics of the system and corresponds to the case where there is no energy barrier ($\Delta F^* = 0$) and equilibration is limited by molecular mobility. The parameter δL is experimentally determined from the initial film height, h_0, using eq. (1) and the equilibrium bilayer spacing measured using AFM. Thus, the incubation time for islands may be calculated for each $(N + 1/2)$ number of layers formed in the metastable state. As well, the identical calculation may be performed for hole, rather than island, nucleation with the same result, the only difference being that δL is a negative quantity, causing a sign change in the exponential of eq. (6). Notice that for a commensurate film where $L = L_0$, $\delta L = 0$, and we recover the expected divergence of the incubation time for commensurate films. Conversely, as the film thickness deviates further from commensurability, δL increases causing a greater driving force to nucleation and a resultant decrease in the incubation time as indicated by eq. (6).

In fig. 3 we plot the experimentally determined incubation time as a function of film thickness, as well as the model with $\tau_0 = 1100\,\mathrm{s}$ and $\beta = 0.1L_0$. Clearly the simple nucleation model, calculated in the SSL, effectively describes the data. As the initial film height approaches commensurability, the model diverges and the measured values increase more than 2 orders of magnitude in comparison to τ_{inc} for incommensurate films. There is little variation in τ_{inc} for incommensurate films regardless of the number of bilayers formed in the metastable state. However, the nearly commensurate films show larger increases in τ_{inc} for thicker films. This difference in commensurability effect on τ_{inc} can be attributed to the fact that bilayers deform less in the metastable state for thicker films, as there are more bilayers to compensate for the incommensurability of the film. Since the bilayers are deformed less, there is a decrease in the driving force to nucleate for thicker films, thus the incubation time is longer. This phenomenon emerges naturally from the model since L, and consequently $\delta L = L - L_0$, is inversely proportional to $(N+1/2)$ according to eq. (1). This inverse proportionality causes a decrease in maximum δL for thicker films, resulting in an exponential increase in eq. (6). This decrease in driving force causes a narrower region of short incubation times as can be seen in the linear inset of fig. 3. We note that this model assumes a homogeneous sample, ignoring any existence of defects. Additionally, the precise pathway by which islands and holes are nucleated is not taken into consideration for our calculations. Thus, it is expected that some of our measured incubation times will be much shorter than predicted, simply due to defects and ordering pathways of the sample which lower the activation barrier to nucleation. Therefore, the model provides an upper bound on the experimental results.

Though our model provides a good description for nearly commensurate films ($h_0 \sim (N + 1/2)L_0$), as the film heights approach complete incommensurability, the assumptions of the model break down. We assumed that the intermediate state consists of equally deformed lamellae as that is the lowest free-energy morphology consistent with our measurements. However, for incommensurate films, the incubation time becomes much shorter and approaches the timescale of the ordering time. As τ_{inc} gets shorter, the intermediate state will take on a morphology which is not only driven by energetics, but kinetics as well. This intermediate state could then be quite different from the assumption of equally deformed layers, altering the ordering pathway and dynamics for island and hole formation. Nevertheless, the model of the ordering pathway provided here for PS-PMMA thin films provides an acceptable description of the data.

5 Conclusions

In summary, using ellipsometry we were able to measure two distinct timescales in the ordering process of symmetric diblock copolymer films before the ultimate formation of islands or holes at the free surface. At 155 °C we observe an increase in τ_{ord} for thicker films which we attribute to the additional time required to order more bilayers in the metastable state. Annealing at 160 °C, incubation times were found to increase by up to 2 orders of magnitude for nearly commensurate films. As well, thicker films demonstrated a stronger dependence of τ_{inc} on commensurability due to a decrease in driving force from bilayer deformation in the metastable state. The nucleation model, based upon the SSL, captures the physics required to describe the incubation time results while providing insight into the metastable morphology of nearly commensurate symmetric diblock films.

Financial Support for this work was provided by National Sciences and Engineering Research Council (NSERC). The authors thank Mark Matsen for helpful comments.

References

1. G.H. Fredrickson, F.S. Bates, Annu. Rev. Mater. Sci. **26**, 501 (1996).
2. I. Hamley, Progr. Polym. Sci. **34**, 1161 (2009).
3. T. Thurn-Albrecht, J. Schotter, G.A. Kastle, N. Emley, T. Schibauchi, L. Krusen-Ebaum, K. Guarini, K.T. Black, M.T. Tuominen, T.P. Russell, Science **290**, 2126 (2000).
4. C. Tang, E.M. Lennon, G.H. Fredrickson, E.J. Kramer, C.J. Hawker, Science **322**, 429 (2008).
5. C. Creton, E.J. Kramer, H.R. Brown, C.Y. Hui, Adv. Polym. Sci. **156**, 53 (2001).
6. P. Mansky, Y. Liu, E. Huang, T.P. Russell, C. Hawker, Science **275**, 1458 (1997).
7. M.J. Fasolka, A.M. Mayes, Annu. Rev. Mater. Res. **31**, 323 (2001).
8. P.F. Green, R. Limary, Adv. Colloid Interface Sci. **94**, 53 (2001).
9. S. Joly, D. Ausserre, G. Brotons, Y. Gallot, Eur. Phys. J. E **8**, 355 (2002).
10. G. Vignaud, A. Bigaud, G. Grubel, S. Joly, D. Ausserre, J.F. Legrand, Y. Gallot, Physica B **248**, 250 (1998).
11. S. Joly, A. Raquois, F. Paris, B. Hamdoun, L. Auvray, D. Ausserre, Y. Gallot, Phys. Rev. Lett. **77**, 4394 (1996).
12. B. Collin, D. Chatenay, G. Coulon, D. Ausserre, Y. Gallot, Macromolecules **25**, 1621 (1992).
13. K.S. Lyakhova, A. Horvat, A.V. Zvelindovsky, G.J.A. Sevink, Langmuir **22**, 5848 (2006).
14. J.L. Carvalho, M.V. Massa, S.L. Cormier, M.W. Matsen, K. Dalnoki-Veress, Eur. Phys. J. E **34**, (2011).
15. R.M.A. Azzam, N.M. Bashara, *Ellipsometry and Polarized Light* (North Holland, Amsterdam, 1987).
16. A. Menelle, T.P. Russell, S.H. Anastasiadis, S.K. Satija, C.F. Marjkrzak, Phys. Rev. Lett. **68**, 67 (1992).
17. K.R. Shull, Macromolecules **25**, 2122 (1992).
18. A.B. Croll, A.C. Shi, K. Dalnoki-Veress, Phys. Rev. E **80**, 051803 (2009).
19. M.J. Fasolka, P. Banerjee, A.M. Mayes, G. Pickett, A.C. Balazs, Macromolecules **33**, 5702 (2000).
20. S. Wu, *Polymer Interfaces and Adhesion* (Marcel Dekker, New York, 1982).
21. T. Russell, Macromolecules **23**, 890 (1990).
22. G.H. Fredrickson, E. Helfand, J. Chem. Phys. **87**, 697 (1987).
23. M. Matsen, J. Chem. Phys **106**, 7781 (1997).
24. A. Semenov, Sov. Phys. JETP **61**, 733 (1985).
25. T.P. Russell, P. Lambooy, G.J. Kellogg, A.M. Mayes, Physica B **213-214**, 22 (1995).